Molecular Crystals and Liquid Crystals Science and Technology. Section A. Molecular Crystals and Liquid Crystals
Publication details, including instructions for authors and subscription information:
http://www.tandfonline.com/loi/gmcl19

The Role of Excitonic Light Collection, Exciton Diffusion to Interfaces, Internal Fields for Charge Separation, and High Charge Carrier Mobilities

N. Karl [a], A. Bauer [a], J. Holzäpfel [a], J. Marktanner [a], M. Möbus [a] & F. Stölzle [a]
[a] 3, Physikalisches Institut, Universität Stuttgart, D 70550, Stuttgart, Germany

Version of record first published: 24 Sep 2006.

To cite this article: N. Karl , A. Bauer , J. Holzäpfel , J. Marktanner , M. Möbus & F. Stölzle (1994): The Role of Excitonic Light Collection, Exciton Diffusion to Interfaces, Internal Fields for Charge Separation, and High Charge Carrier Mobilities, Molecular Crystals and Liquid Crystals Science and Technology. Section A. Molecular Crystals and Liquid Crystals, 252:1, 243-258

To link to this article: http://dx.doi.org/10.1080/10587259408038230

Mol. Cryst. Liq. Cryst. 1994, Vol. 252, pp. 243–258
Reprints available directly from the publisher
Photocopying permitted by license only

Printed in the United States of America

EFFICIENT ORGANIC PHOTOVOLTAIC CELLS

The Role of Excitonic Light Collection, Exciton Diffusion to Interfaces, Internal Fields for Charge Separation, and High Charge Carrier Mobilities.

N. KARL, A. BAUER, J. HOLZÄPFEL, J. MARKTANNER, M. MÖBUS, F. STÖLZLE
3. Physikalisches Institut, Universität Stuttgart, D 70550 Stuttgart, Germany

Abstract Organic photovoltaic thin film structures made by vacuum vapor deposition have been studied. From the spectral response as a function of the absorption coefficient we conclude that electron–hole generation takes place at the interface between the organic thin film and one or both of the semitransparent cover electrodes. The observed short circuit currents, however, are too large to be explained on the basis of a *direct* light-induced charge transfer at the organic thin film/electrode interface. Rather, a contribution of the bulk-absorbed photons is necessary to account for the observed quantum yield. Transfer of the energy to the interface sites can be explained by diffusional migration of excitons. The efficiency of charge separation can be improved by combining donor and acceptor type partners in organic double layers. The efficiency of *power* conversion, however, not only depends on a suitable choice of the absorption spectra and of the ionic energy levels of the materials employed, but also on the internal cell resistance, a fact that calls for high charge carrier mobilities, and hence for using materials with crystal structures that allow strong π-electron interactions, and for deposition in high chemical purity and structural perfection.

Keywords: photovoltaic, electron donor, electron acceptor, electron-hole generation, p-type, n-type, exciton diffusion, mobilities, charge separation

INTRODUCTION

It is a common feature of all solids that excitation by electromagnetic radiation of sufficient photon energy can lead to ionization of the constituent atoms or molecules and thus induce or increase internal (bulk) conductivity or emit electrons across a surface or interface (external or internal photoemission).

The light-induced electron–hole generation and separation is an important process not only for light detection and measurement (photocells), but also for conversion of light to electric or even chemical energy (solar cells; photosynthesis), the latter being the basis of all life on earth.

The reverse process, electron–hole recombination, frequently leads to

light generation, known as electro or (charge carrier-)injection luminescence, a field currently under very intense investigation for both, inorganic and organic solids.

Electrical conductivity in organic solids is mainly based on substances that carry conjugated π-electrons, such as the homo- and heteroaromatics and the polyenes.

Our studies, to be presented here, basically aim at a better understanding of the fundamental processes involved in electron–hole pair generation and separation in *organic thin film sandwich structures*. In addition, it is expected that conclusions can also be drawn on some details of radiative and nonradiative electron–hole recombination.

Historically the topic dates back to as early as 1913, when M. Volmer at the University of Leipzig reported on the first organic solid state photocell made by fusing a thin anthracene ($C_{14}H_{10}$) layer between two platinum contacts on a glass substrate and adding a thin paraffinic protective cover layer against the attacks of oxygen and water vapor[1].

After a long period of silence literature focussed on *photoconductivity* of (thin) organic crystals. For electrolytic electrodes, which were frequently applied, two surface generation processes could be distinguished: I) a spectrally sensitized photoconduction based on charge transfer from directly excited surface-adsorbed dye molecules, and II) a yield-sensitized photoconduction based on bulk light absorption, exciton diffusion to the interface, and disproportionation into an electron–hole pair at surface-adsorbed ions or dye molecules, (Steketee, de Jonge, 1962, 1963)[2,3]. Similar experiments were performed later by Karl and Schmid under cleaner conditions, using an in situ vacuum vapor-deposited sensitizing layer and Kepler - LeBlanc type pulsed photoconductivity measurements in a capacitive electrode arrangement[4].

A nonlinear exciton–exciton annihilation process was identified as the main source of *bulk* charge carrier generation near the optical absorption edge (cf. discussion and references given by LeBlanc, 1967)[5], whereas a process linear in the light intensity was usually found only for photon energies about one eV higher (Castro and Hornig, 1965)[6]. The bulk light-induced initial ("geminate") electron–hole pairs resulting of either process are not yet free to move independently, but are still mutually bound by ≈ 0,5 ... 1 eV by their Coulombic attraction. Their final separation under stochastic diffusional and electric field driven directional motion, in competition with the concomitant recombinative backreaction has been treatet by Batt, Braun and Hornig 1968[7] (by adaption of a model initially devised by Onsager to describe similar *ionic* processes in electrolytes[8]). Typical zero electric field quantum yields in the crystals studied (e.g. anthracene) amounted to no more than $\approx 10^{-4}$ electrons per absorbed photon.

Electrophotography people, however, succeeded to develop composit polymer foils that reach quantum yields near 1 under the exceedingly high fields ($\sim 10^6$ V/cm) applied in this technique (see e.g. ref. 9). These devices are in widespread use nowadays.

Photovoltaic response of organic crystals and thin films was studied occasionally[10-17], but did not find great publicity because of very small efficiency, until Gosh and Feng 1978[18,19] reported on an Al/merocyanine/Ag single organic layer, and Tang 1986[20] on a In_2O_3/Cu-phthalocyanine/perylene-pigment/Ag double organic layer photovoltaic cell that reached 0.7% and $\sim$ 1% power conversion efficiency under simulated AM1 and AM2 solar illumination, respectively. For a review of the field the references 21 and 22 may be consulted.

Concerning the prospect of such findings for further developments into potential practical applications, an important question — among many others to be solved — has been, whether for such kind of organic thin film photovoltaic cells the initial electron—hole pairs are generated essentially in the bulk, or rather at one of the surfaces in contact with an electrode (or at the organic/organic interface in the case of two different organic layers). And, given the surface/interface version was correct, whether then only the small fraction[§]) of photons absorbed in the immediate neighbourhood of such a discontinuity can lead to charge carriers (what would have supported the scepticism of the critics who doubted that a reasonable, practically relevant zero bias quantum efficiency could be obtained with organics at all) — or whether the absorbed light energy could be harvested more efficiently by involving more distant absorbing molecules and making use of energy transfer by diffusively mobile excitons to places where disproportionation into positive and negative moieties and spatial separation by a built-in field can take place.

Nature, obviously, has anticipated such ideas in the architecture of the photosynthetic units by employing antennae molecules and energy transfer, in order to lend more efficiency to the photosynthetic process.

THEORETICAL CONSIDERATIONS

It is obvious that efficient photovoltaic power conversion requires a generation process linear in the light intensity and that it cannot be based on a homogeneous bulk generation of electrons and holes. A continuous linear bulk generation process would require band to band transitions for which the necessary photon energy is considerably higher than the absorption edge and the (zero field) quantum yield is low. More seriously, there would be additional non-geminate recombination losses and no directional driving force. Generation of an inhomogeneous charge carrier pair distribution, as an alternative,

§ Typical minimal absorption lengths are $3 \cdot 10^{-6}$cm $\hat{=}$ 30...100 molecular layers.

can cause an EMF as a consequence of different electron and hole diffusion velocities along the concentration gradient; this so called "Dember effect" (cf. ref. 17 ch.II-G and ref. 28) is not very efficient, however, concerning power yield.

It is therefore necessary that a suitable Schottky-barrier type space charge distribution is built in that produces a high separating electric field. A large difference of the Fermi levels of the two materials to be contacted is thus of prime importance. Generation of charge carrier pairs at the Schottky barrier interface (or within a small interaction radius) can be based on direct light absorption in this area, or on excitation energy diffusing in as excitons, created further apart, outside the space charge field region, and desintegrating at the barrier. For describing the latter process, the very general derivation given in ref. 27 ch. I-G8 can be used:

Let us assume that the surface at $x = 0$ is illuminated and the Lambert–Beer law of light absorption holds, with an absorption coefficient α, equivalent to an absorption length $L_A = \alpha^{-1}$, for a given photon wavelength λ (energy $h\nu$) and principal polarization direction; let us further assume a finite diffusion length L_D and a diffusional velocity v_D for the created excited state S^* of lifetime τ, defined as $L_D = \sqrt{D\tau}$ and $v_D = D/L_D = L_D/\tau$, a finite sink of the exciton concentration at the interface at $x = 0$, characterized by a recombination velocity v_r into the sink, and, finally, a quantum yield η_{cc} for the net reaction at the sink into the charge carrier channel $S^*(x=0) \rightarrow e + p$; then the dependence of the reaction yield η (number of charge carriers per second and cm^2 delivered into the short circuit current per total absorbed photons per second and cm^2) on the absorption length can be derived as an analytic expression (cf. ref. 19): Under the assumption of a sample thickness $L \gg L_A$ this expression can be simplified[27] to

$$\eta^{-1} = \eta_{cc}^{-1}\left(1 + \frac{v_D}{v_r}\right)\left(1 + \frac{L_A}{L_D}\right) \qquad (1)$$

(where the recombination velocity v_r has been defined by the differential equation $D(dS^*/dx) = v_r S^*$ at $x = 0$). A plot η^{-1} versus $L_A = \alpha^{-1}$ should therefore give a straight line yielding the (average) diffusion length L_D of the excitons as the ratio of ordinate intercept to slope, or, equivalently, as the negative intercept of the continued line on the abszissa, $-L_A(\eta^{-1} = 0) = L_D$. For lack of better knowledge we shall assume ideal exciton sinks at the electrodes, i.e. $v_r \gg v_D$. Then η_{cc}^{-1}, the yield of the exciton decay at the Schottky barrier into the charge carrier channel, can be read off as the ordinate intercept at $L_A = 0$. A full expression, valid also for L_A and L_D comparable to the sample thickness L, meaning that excitons can also reach the rear electrode and create charge carriers there, may be found in ref. 19.

EXPERIMENTAL

Glass slides, $32 \times 20\,mm^2$, partially covered with a conductive indium/tin oxide (ITO) electrode layer of ~80% transmittance in the visible and $\sim 300\,\Omega\,\square$ area resistivity were cleaned and outgassed by heating at 450K under a vacuum of 10^{-4} Pa before vapor deposition of the desired material onto the substrate (held at a preselected temperature between 210K and 470K) from a tiny indirectly heated Ni crucible (cf. ref. 23) whose temperature was controlled via a thermocouple formed with a Ni and a NiCr wire welded on. The starting materials for thermal vacuum vapor deposition were obtained from commercially available perylene-3,4,9,10-tetracarboxylic-3,4,9,10-dianhydride (PTCDA, $C_{24}H_8O_6$), naphthalene-1,4,5,8-tetracarboxylic-dianhydride (NTCDA, $C_{14}H_4O_6$) H_2-phthalocyanine (H_2Pc, $C_{32}H_{18}N_8$), diindeno[1,2,3-cd,1',2',3'-lm]perylene (DIP, $C_{32}H_{16}$), and perylene (Pe, $C_{20}H_{12}$)) after purification by temperature gradient sublimation in a weak N_2 gas stream at ~10 Pa. PTCDA and NTCDA are acceptor-type molecules, distinquished by a comparatively large solid state electron affinity (A), whereas H_2-Pc, DIP and Pe are donor-type molecules with small solid state ionization threshold energies (I_s)[24-26]. Typical sublimation temperatures used for making the thin films were around 670K (PTCDA and H_2Pc), 650K (DIP), 540K (NTCDA), and 500K (Pe), fine-adjusted such that the deposition rate, monitored by a quartz oscillator balance, was ca. 0.1nm/min. In a last step a typically T = 20% Ag electrode film was vapor-deposited through a subdivided shadow mask, leading to 16 independent $0.18\,cm^2$ cells on each substrate; the Ag thickness was controlled by monitoring the transmission for a $\lambda = 670\,nm$ light beam from a diode laser.

The measurement apparatus consisted of a 150W XBO lamp, a chopper (35Hz), a water heat filter, a f = 25cm f/4 grating monochromator equipped with a digital angular encoder, and a variable (wedged) neutral density filter (NDF) - both driven by stepping motors —, selectable edge filters and a lock-in amplifier. A computer (AT) was employed for wavelength selection and scanning, for measuring photocurrents and photovoltages, and for steering the NDF in such a way that the photon flux density onto the photocell under examination was kept constant (at a preselected value between $7 \cdot 10^{12}$ and $1 \cdot 10^{14}\,s^{-1}cm^{-2}$ at $\Delta\lambda = 20\,nm$) during a wavelength scan. (This measure is important for comparison and indispesable in case of nonlinear response). Time resolved measurements were made by excitation by 0.9ns, 150kW light pulses from a home-made nitrogen laser ($\lambda = 337\,nm$), or 0.5ns, 20kW light pulses from a tunable dye laser, pumped by the former, and recording on an oscilloscope. For current/voltage and capacitance/voltage measurements an oscillographic x — y technique was used, with the driving AC voltage fed to the x-deflection plates and the resulting current signal — after an impedance transformation by an operational amplifier — to the y-plates.

RESULTS

single layer cells

Typical measured photovoltaic response curves for ITO/PTCDA/Ag cells are shown in the figs. 1 and 2. Under the conditions given in the caption, the short circuit currents, j, exhibited a slightly sublinear dependence on the light intensity, I, with $j \sim I^n$, with $0.8 \leq n \leq 1$ for one order of magnitude intensity reduction. For the higher light intensity of the full spectrum a stronger sublinearity until $n \approx 0.5$ was obtained. For the Ag/PTCDA junctions studied the dependence of the short circuit current j_{sc} on the open circuit voltage U_{oc} obeyed a $j_{sc} = j_o[\exp(eU_{oc}/nkT) - 1]$ law, typical of Schottky diode photovoltaic cells, with a quality factor of $n = 1.1$. Open circuit voltages up to 0.4 V were found. With a cell operated under an external AC bias typical *diode* j/U characteristics were obtained, whith an increase of the currents under illumination. Capacitance/voltage, C/V, measurements gave bias-dependent capacitances for frequencies up to 100 Hz with $C^{-2} \sim U_{bi} - U$ (where U_{bi} is the *built in* voltage, caused e.g. by an internal bipolar space charge, responsible for band bending as a consequence of Fermi level adjustment). For Ag/PTCDA/ITO a charge carrier density in the space charge of $10^{17}\,cm^{-3}$ and a potential barrier $U_{bi} \approx 0.7$ V were derived, leading to an estimate of the width of the space charge layer of 40 nm and a field of $2 \cdot 10^5$ V/cm (in another independent sample these values were $4 \cdot 10^{17}\,cm^{-3}$, 0.6 V and 15 nm. Pulsed photocurrent measurements ($\lambda = 540$ nm) with a Ag/1μmPTCDA/ITO cell illuminated through the silver electrode detected electrons as the mobile charge carriers in PTCDA, with a biexponential decay; the shorter time constant, possibly due to (at least intermediate) capturing of free electrons by shallow traps, amounted to 200 ns, the longer component had a lifetime of several ms.

From fig. 1 and 2 it can be seen that the photocurrent excitation spectrum parallels the optical absorption spectrum – cf. fig. 5a, dashed curve – (which is occasionally called a "symbatic" behaviour) for illumination through the Ag electrode (full symbols), but displays a minimum at maximal absorption and maxima for weak absorption at the wings of the absorption spectrum when light is admitted from the ITO side ("antibatic" behaviour; open symbols). This minimum becomes more pronounced as the layers get thicker, until finally only a response is measured near the absorption edges at 600 and at 400 nm; only for very thin PTCDA layers, comparable to the absorption length, which we had difficulties to produce free of pinholes with a reasonable probability, the cells became essentially symmetric, see fig. 2. These findings suggest that the Ag electrode is the active one and *electrons* are injected into the PTCDA from this active electrode, in accordance with what was found with the pulsed measurements. Occasionally, however, even a slightly negative current was observed for the thinner samples, and, very rare-

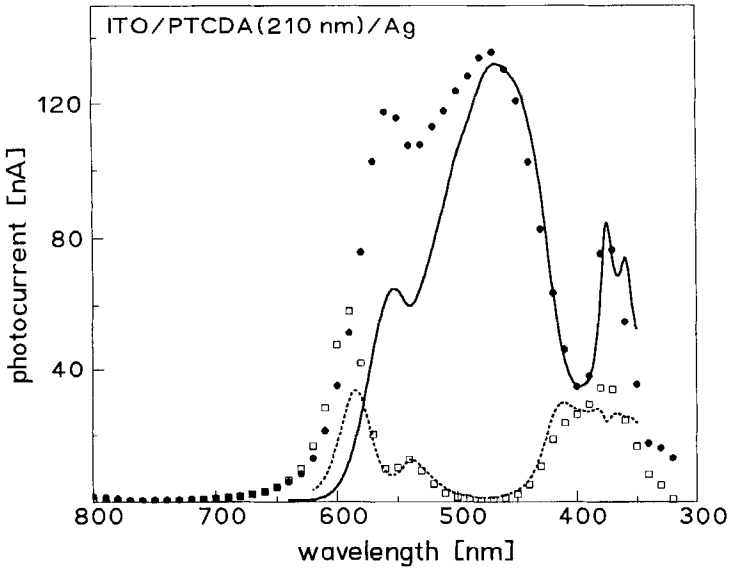

Fig. 1 Typical measured excitation spectra of the short circuit photovoltaic current delivered by a Ag/PTCDA/ITO sandwich cell upon illumination by $6 \cdot 10^{13} h\nu/cm^2 s$ ($\Delta\lambda = 20$ nm) through the silver electrode (full symbols) and through the ITO electrode (open symbols) The full and the dotted line in fig. 1 are calculated with eq. (1).

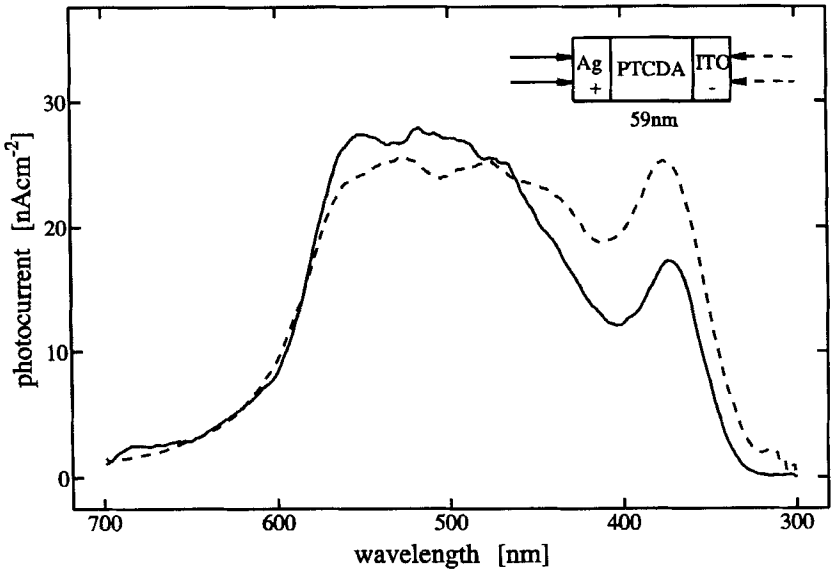

Fig. 2 Short circuit photovoltaic current as a function of wavelength for a 59 nm PTCDA layer and excitation through either the Ag (full line) or the ITO electrode (dashed line); $9 \cdot 10^{12} h\nu/cm^2 s$.

ly, the ITO electrode was fully active in injecting electrons when illuminated, cf. fig. 4. (The current is always counted positive when the silver electrode assumes a more positive potential than the ITO electrode).

It is unclear why there is considerable statistical scatter in the response when illuminating through the ITO; although its Fermi level is very close to that of Ag it acts as a photovoltaically active electrode only occasionally. In addition, the magnitude of the photocurrent density greately varied from batch to batch and even from cell to cell in the same batch. This has probably to do with poor reproducibility of the microscopic structural properties and with contaminations of the layer and the electrodes; the latter calls for working under UHV conditions. However, it can clearly be stated that the illuminated Ag or ITO electrode, if active, always acted as an electron injetor into PTCDA. Similar findings were made with NTCDA. Both molecules are fairly strong electron acceptors, due to the 6 oxygen atoms in their anhydride rings. In contrast, *holes* were always found to be injected from a *photoactive* Ag or ITO electrode into the donor-type materials investigated, H_2Pc, Pe, DIP and TTBT but the photovoltaic response of these systems was usually low and often even Ohmic contacts were obtained.

Typical *particle* or *number quantum yields* (electrons/s in the outer circuit per photons absorbed in the organic layer) amounted to between a few% and ~20%. Technical *power yield* (electrical power extractable per total incoming light power per cm^2, however, was always low (on the order of 10^{-3}). This is obviously due to high internal resistance and recombination losses. Since the investigations to be presented here aimed at solving some of the more principal problems, we did not yet try to optimize the power yield.

A plot of the inverse short circuit current yield against the light penetration depth or inverse absorption coefficient measured for a PTCDA sample, fig. 3, leads to a straight line, as predicted by the proposed model expressed by eq. (1). Several such curves have been obtained with different samples made with the same and with different organic materials and found qualitatively similar. An interesting example of the rare case of a Ag/PTCDA/ITO cell with *both* electrodes photoactive is presented in fig. 4. With a layer thickness of 130nm the cell is optically dense and thicker than the exciton diffusion lengths typically found in PTCDA; upon illumination the Ag and the ITO side are therefore independent. It is remarkable that the exciton diffusion lengths evaluated for the two sides are markedly different: that at the ITO side is much larger (44nm) than that at the Ag side (12nm), whereas the particle quantum yield η is nearly the same for both sides (9.7% and 13%, respectively). This observation seems to indicate that the structural quality of the organic layer is better near the solid substrate where the first PTCDA molecules arrived and probably formed a fairly ordered structure initially, after all what is known from the different structural investigations with

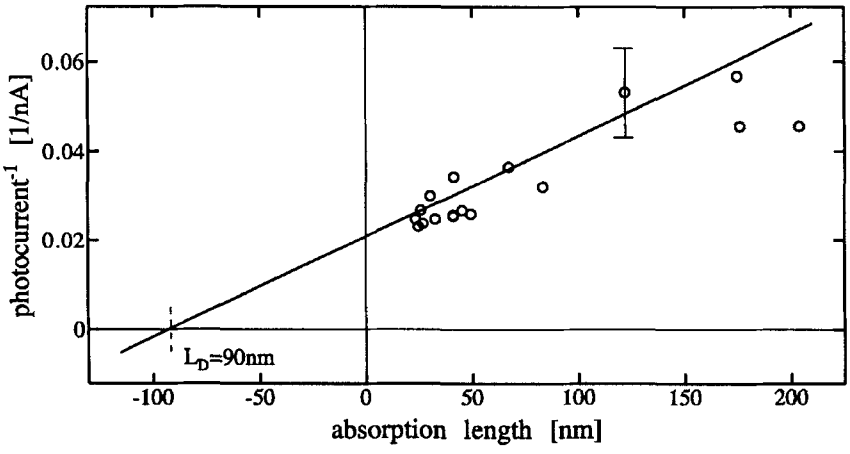

Fig. 3 Photocurrent of a representative Ag/PTCDA/ITO photocell illuminated through the Ag electrode, as a function of the absorption coefficient at different wavelengths; plot 1/j versus $L_A = 1/\alpha$. In this representation the regression line yields an exciton diffusion length $L_D \approx 90$nm and a particle quantum yield $\eta_{CC} \approx 3\%$.

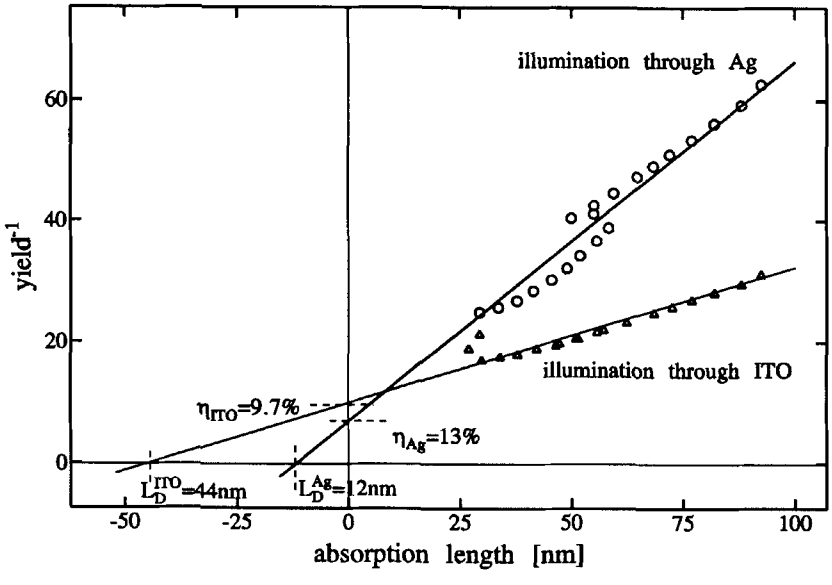

Fig. 4 Dependence of the photocurrent yield η on the light absorption length for the rare case of a Ag/PTCDA/ITO photocell for which not only the Ag electrode was photoactive, but also, with a very similar response, the ITO electrode; plot $1/\eta$ versus $L_A = 1/\alpha$ for both electrodes. A larger exciton diffusion length (44nm) is found at the ITO electrode which is the substrate onto which the film (130 nm) was vapor-deposited.

vapor-deposited PTCDA layers on different substrates.

Double layer cells

The finding that the donor or acceptor character of the molecules determined the sign of the injected carriers lead us to the idea to try donor/acceptor

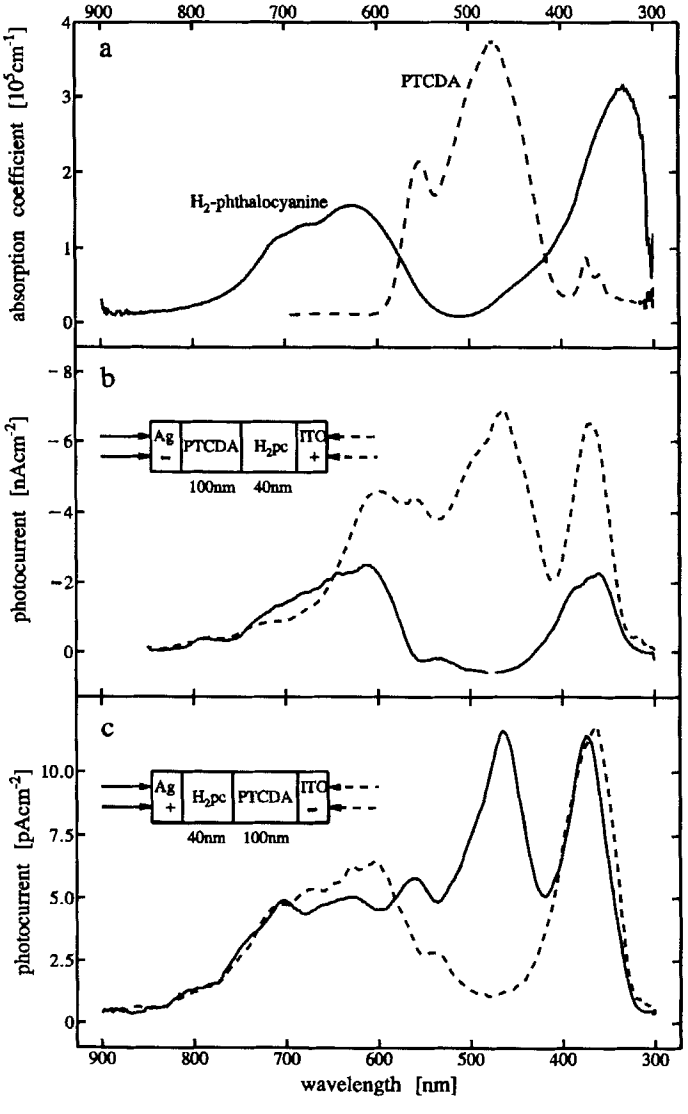

Fig. 5 Absorption spectra of 150 nm vapor-deposited PTCDA and H_2Pc layers (a), and photovoltaic short circuit current action spectra for 100 nm PTCDA / 40 nm H_2Pc double (organic) layer cells with normal and reversed Ag and ITO electrode configurations, (b) and (c), illuminated through the Ag and through the ITO electrodes. The nonoverlapping absorption spectra allow to distinquish at which interface the charge carriers are generated.

double layer combinations and to check if efficient charge separation can be obtained upon light absorption at or exciton diffusion to the internal organic/organic interface, with the electrons flowing into the acceptor, the holes into the donor layer. In the classical p/n semiconductor photodiode picture such a process can be expected to occur if the Fermi levels of the two layers differ sufficiently and with the appropriate sign of the difference, and if charges are able to separate and flow over the boundary to adjust the Fermi levels by building up a space charge double layer.

Fig. 5 displays results obtained with the double layer structures Ag/PTCDA/H_2Pc/ITO and Ag/H_2Pc/PTCDA/ITO (reverse order) upon illumination through the Ag or the ITO electrode, together with the optical absorption spectra. It is observed that the short circuit current photovoltaic response is always more or less antibatic to the absorption spectrum of the layer through which light is admitted. Further, the current sign (with respect to the reference electrode, Ag) depends on the order of the organic layers, but not on the side that is illuminated.

A similar behaviour was observed with DIP/PTCDA as well as with perylene/NTCDA double layer configurations (with the same electrodes as above); a typical result for one order of the layers of the latter system is shown in fig. 6. The absorption edge of NTCDA is at ≈400 nm, with a spectral window between 350 nm and 240 nm, that of perylene at ≈480 nm (with no spectral window between 400 and 350 nm).

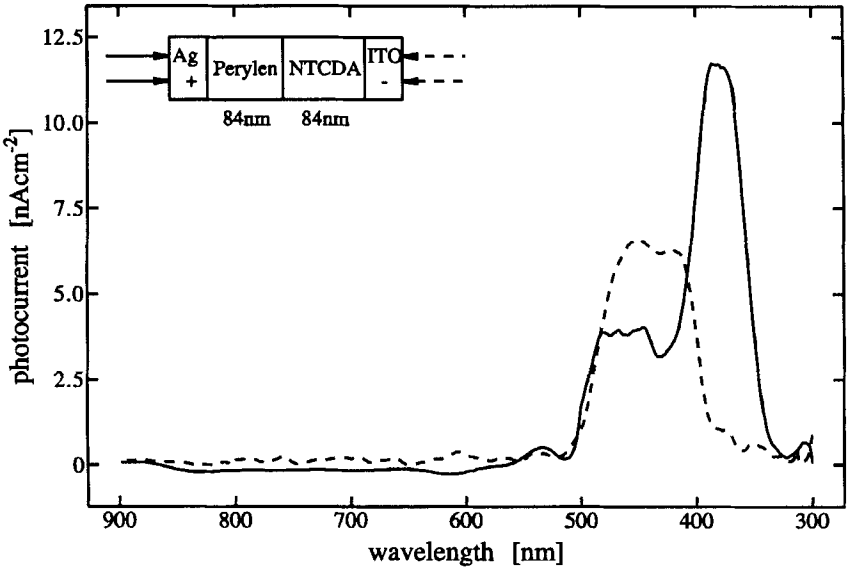

Fig. 6 Photovoltaic short circuit current action spectra of a Ag/Pe/NTCDA/ITO cell ($9 \cdot 10^{12}$ hν/cm^{2}s); corrected for the wavelength-dependent absorption losses in the electrodes. Charge carrier generation occurs predominantly at the organic/organic interface.

DISCUSSION

For tutorial reasons theoretical steady state exciton concentration profiles were calculated for constant illumination through x = 0 and for the boundary conditions S = 0 at x = 0 and at x = L using the analytical expressions of ref. 19; these profiles are displayed in fig. 7. The exciton diffusion currents are determined by the slope of these concentration profiles.

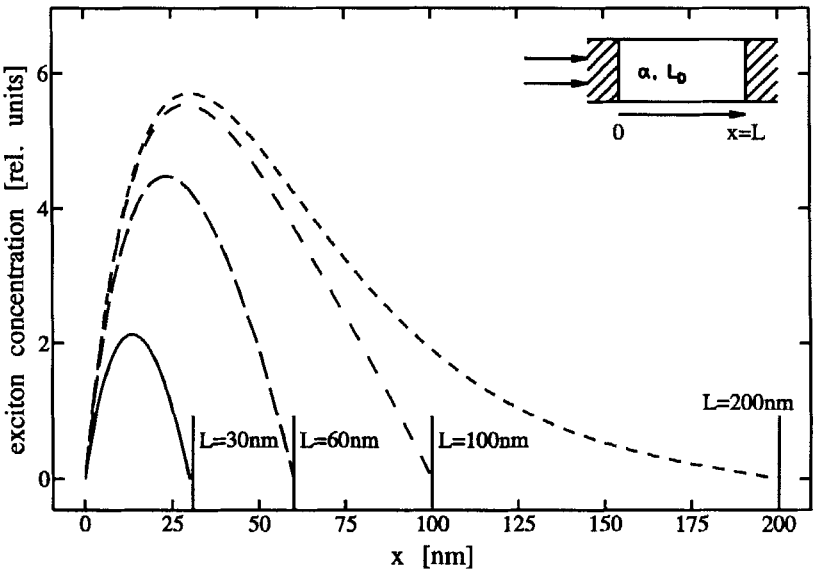

Fig. 7 Exciton concentration profiles for an optical absorption length $L_A = 1/\alpha = 30\,nm$ ($\alpha = 3.3 \cdot 10^5\ cm^{-1}$), an exciton diffusion length of $L_D = 30\,nm$, and different values of the sample thickness L. The illuminated side is at x = 0. For $L_A \approx L_D \approx L$ the excitons reach the rear surface nearly as efficiently as the front surface.

The exciton concentration profile becomes essentially symmetric for a sample thickness comparable to the absorption length. As can be seen from fig. 2, the photocurrent is then essentially independent of which side is illuminated, that with the active or that with the inactive electrode. If only the light quanta immediately absorbed at the molecular layer adjacent to the electrode were active, the response of the 59 nm cell should have been reduced to ca. $1/e^2$ upon illumination through the ITO electrode, which is not the case and, thererefore, is in favour of the exciton diffusion model.

More evidence is gained by a quantitative consideration of the (particle) quantum yield expected if only light absorbed locally in a monomolecular layer adjacent to the electrode was active in producing charge carriers (e.g. by a charge transfer reaction across the interface to the electrode) and no

exciton diffusion was involved: It follows from the crystal structure of PTCDA[29] that a monolayer is ≈ 1.2 nm thick at best, leading to a maximal fraction of absorbed photons $dI/dx = \alpha \cdot x = 3.6 \cdot 10^{-3}$ for $\alpha = 3 \cdot 10^5 cm^{-1}$, in strong contrast to the observed 10% and more electrons per photon absorbed in the organic layer, even if the quantum yield η_{cc} for exciton decay into the charge carrier channel was 1, which is unlikely.

A further, more crucial test of the applicability of the exciton diffusion model would be to check, whether the functional dependence of the photocurrent on the absorption coefficient obeys eq. (1). We have made such plots with the data obtained for a number of PTCDA cells (examples were given in the figs. 3 and 4), and also for some cells made with the other organic materials mentioned, and found that the experimental points could be fitted satisfactorily by a straight line with a negative intercept on the abscissa in all cases, although the scatter was sometimes large. Extrapolated exciton diffusion lengths also displayed considerable scatter, ranging from between several nanometers to 90 nm for PTCDA, to 25 nm for DIP, and to 10 nm for NTCDA. In view of the fact that singlet exciton diffusion lengths of several ten to more than 100 nm have been measured in well purified organic single crystals such as anthracene[2,30], tetracene[31], and phenanthrene[32], these numbers appear reasonable.

In addition, the exciton diffusion model is also strongly supported by the fact that measured photocurrent action spectra and spectra predicted by calculations, that require only the absorption spectrum, agree fairly well, cf. fig. 1.

The antibatic behaviour of the photocurrents in the double layer cells indicates that generation of charge carriers there always occurs with filtered light. In comparison with the single layer cells the sign of the net generated photovoltage is reverse, the electrode on the acceptor type material becomes negative, the electrode on the donor type material positive. If there are responses at the electrodes as well, as in the single layer cells, which is reasonable to assume, then these are obviously overbalanced by an opposite photo-emf that can only have its origin at the organic/organic interface, in perfect agreement with the observed antibatic behaviour: the optimum (symbatic) effect is always obtained for light that enters through a spectral window of the other layer to reach the organic/organic interface. (The H_2Pc/PTCDA system was chosen to allow these distinctions to be made). The overbalancing indicates that the photovoltaic effect at the organic/organic junction is always larger than the effects at the electrodes.

The sign of the emf generated at the organic/metal and organic/organic interfaces in conjunction with knowledge about the ("ionic") energy levels of the organic materials should enable one to conclude the mechanism of charge carrier creation and separation. From solid state ionization threshold energies

and electron affinities of these and comparable molecules one has to conclude that the Fermi levels of these organic materials, if they are intrinsic, should lie above (i.e. at smaller electron binding energy than) those of Ag or ITO for the donor-type molecules, and below for acceptor-type molecules. Adjustment of Fermi levels then would require that the donor-type material takes up a positive charge, the acceptor-type material a negative charge, to bend the bands down and up, respectively. These fields, however would act *against* the direction of charge carrier separation that is actually observed.

Thus one is obliged to conclude that the internal fields are actually in the direction opposite to what one would expect under the assumption that these organic semiconductors were intrinsic. This requires that *all* materials considered here should be heavily doped, the acceptor-type materials by "strong" donors, i.e. donors with a small electron binding energy, the donor-type materials by strong acceptors. The same argumentation holds for the organic/organic interfaces, where also the polarity of the observed responses is just opposite to what would be expected with intrinsic materials on the basis of classical semiconductor band bending pictures, and where, therefore, also a strong doping has to be assumed.

But why should a wide bandgap donor type material be strongly acceptor-doped and vice versa, with even a cross over of the Fermi levels of the donor and the acceptor type materials? Whereas this might perhaps be feasible at a donor - acceptor junction by interdiffusion of the molecules and differences in the polarization energies, it is difficult to explain for the metal/organic semiconductor interfaces. While it is obvious from classical semiconductor theory that p-n junctions form internal fields that separate the charge carriers and prevent recombination, and that determine the maximum voltage obtainable (the difference of the Fermi levels, or approximately the band gap), it does not seem to be clear at all, what role internal fields play in organic photovoltaic cells, how they are built up and what determins or limits the potential drop across them. The maximum built-in potential difference is certainly also the limiting factor of open circuit voltage for organic cells. There is clearly a need for further and more detailed basic investigations on the energy levels and internal fields as well as for studies with actual photocell units. It is not unlikely that the internal fields are at least to some extent generated by trapped space charge, rather than by donors and acceptors.

Finally a few remarks are due, concerning power yield. To obtain a reasonable power yield, and to possibly compete with inorganic devices, all the parameters discussed above would have to be optimized: Use highly absorbing materials with short absorption lengths in the appropriate spectral region; this is clearly a domain of organic dyes; use strongly interacting molecules for large exciton diffusion constants; select molecules with a long exciton lifetime and low fluorescence losses; provide the appropriate energy levels, in-

ternal fields, reaction centers and electrodes, and, maybe - well dosed - suitable local trapping centers — for obtaining a high particle quantum yield.

But that is only one face of the coin. In order to extract high *power,* large open circuit voltages are crucial, which again requires materials and systems to be optimized. Last but not least, the power that can be generated is wanted outside the cell. The internal resistance therefore should be as low as possible. This is the domain of charge carrier mobility and trapping. Whereas high mobilities and little residual trapping have been obtained for a few selected single crystals of high purity and structural perfection[33] the same task is still unsolved for organic thin films. However, recent progress in the field of preparation and characterization of organic thin films and epitaxial layers under well defined and clean conditions, including ultra high vacuum environment and techniques, may give confidence and justify a realistic optimism that much better organic photovoltaic cells than available presently will be feasible in future.

ACKNOWLEDGMENT

We are very grateful for a kind gift of a sample of PTCDA of special purity by Prof. Dr. H. Langhals, University of München. This work has been supported by the Deutsche Forschungsgemeinschaft in the SFB 329 Collaborative Research Center. Partial support by the Fonds der Chemischen Industrie is gratefully acknowledged.

REFERENCES

1. M. Volmer, Ann. Phys. 40, 775 (1913)
2. J.W. Steketee and J.deJonge, Philips Res. Rep. 17, 326 (1962)
3. J.W. Steketee and J.deJonge, Proc. Koninkl. Nederl. Akad. van Wetenschappen - Amsterdam, B66, 76 (1963)
4. N. Karl and E. Schmid (1973); see N. Karl, Adv. Solid State Phys. 14, 261 (1974), Fig. 7; E. Schmid, Dissertation, Univ. Stuttgart (1974)
5. O.H. LeBlanc, Jr. in Phys. and Chem. of the Organic Solid State, Vol. I, D. Fox, M.M. Labes, A. Weissberger, eds. (J. Wiley, New York 1967), p.133
6. C. Castro and J.F. Hornig, J. Chem. Phys. 42, 1459 (1965)
7. R.H. Batt, Ch.L. Braun, and J.F. Hornig, Appl. Opt. Suppl. 3 Electrophotography 20 (1969); see also: idem, J. Chem Phys. 49, 1967 (1968)
8. L. Onsager, Phys. Rev. 54, 554 (1938)
9. Z.D. Popovic, R.O. Loutfy, and Ah-Mee Hor, Can. J. Chem. 63, 134 (1985)
10. R.C. Nelson, J. Opt. Soc. Am. 46, 13 (1956)
11. R.C. Nelson, J. Chem. Phys. 29, 388 (1958)
12. D. Kearns and M. Calvin, J. Chem. Phys 29, 950 (1958)
13. Kallmann and M. Pope, J. Chem. Phys. 30, 585 (1959)
14. H. Baba, K. Chitoku, and K. Nitta, Nature 177, 672 (1959)

15. D. Kearns, G. Tollin, and M. Calvin, J. Chem. Phys. 32, 1020 (1960)
16. H. Inokuchi, Y. Maruyama, and H. Akamatu, Symposium on Electrical Conductivity in Organic Solids, (Interscience Publ. 1961), p.69; idem, Bull. Chem. Soc. Japan 34, 1093 (1961)
17. Yu.I. Plotnikov and Zh.I. Matalygina, Sov. Phys. Solid State 2, 2244 (1961)
18. D.L. Morel, A.K. Ghosh, T. Feng, E.L. Stogryn, P.E. Purwin, R.F. Shaw, and C. Fishman, Appl. Phys. Lett. 32, 495 (1978)
19. A. K. Ghosh and T. Feng, J. Appl. Phys. 49, 5982 (1978)
20. C.W. Tang, Appl. Phys. Lett. 48, 183 (1986)
21. G.A. Chamberlain, Solar Cells 8, 47 (1983)
22. D. Wöhrle and D. Meissner, Adv. Mater. 3, 129 (1991)
23. N. Sato, K. Seki, and H. Inokuchi, Rev. Sci. Instr. 58, 1112 (1987)
24. N. Karl in Landolt-Börnstein, New Series, Group III subvolume 17i, O. Madelung, M. Schulz, H. Weiss eds., (Springer Verlag, Berlin 1985) p.106
25. N. Karl and N. Sato, Mol. Cryst. Liq. Cryst. 218, 79 (1992)
26. N. Sato, H. Inokuchi, B. Schmid, and N. Karl, J. Chem. Phys. 83, 5413 (1985)
27. M. Pope and Ch. E. Swenberg, Electronic Processes in Organic Crystals, (Oxford Univ. Press, New York 1982)
28. N. Karl, Dissertation, (Univ. of Freiburg/Brg., Germany, 1968)
29. A.J. Lovinger, S.R. Forrest, M.L. Kaplan, P.H. Schmidt, and T. Venkatesan, J. Appl. Phys. 55, 476 (1984)
30. R.G. Kepler in: Treatise on Solid State Chemistry, N.B. Hannay ed., Vol.3 (Plenum Press 1976) p. 615
31. G. Vaubel and H. Baessler, Mol. Cryst. and Liq. Cryst. 12, 47 (1970)
32. D. Haarer and G. Castro, J. Luminesc. 12/13, 233 (1976)
33. N. Karl, in Defect Control in Semicondutors, K. Sumino, ed., (North Holland, Amsterdam 1990) p. 1725